MEASUREMENT AND CORRECTION OF DISPERSION IN THE VUV-FEL

E. Prat, W. Decking, T. Limberg, DESY, Hamburg, Germany

Abstract

Increase in transverse beam size in the undulator caused by dispersive effects is one of the major limitations for the operation of FLASH, the VUV-FEL at DESY. Spurious dispersion is caused by field errors and stray magnet fields in the undulator beam line as well as rf coupler kicks, magnet misalignments and field errors in the linac upstream. The impact of these errors on spurious dispersion depends on the actual operating conditions of the accelerator, so it must be measured and controlled frequently. In this paper we present numerical studies of spurious dispersion generation, dispersion measurements and correction results.

INTRODUCTION

FLASH, i.e., **F**ree electron **LAS**er in **H**amburg, is a Vacuum-Ultra-Violet FEL user facility at DESY and a pilot project for the European XFEL [1].

A schematic layout is shown in Figure 1. Electron bunches with a nominal charge of 1 nC are generated in a laser-driven rf gun. Presently, the electron beam can be accelerated to 700 MeV in five TESLA modules. The electron bunches are longitudinally compressed in two bunch compressor chicanes to reach the necessary peak currents for the SASE process. The dog-leg is a collimation section to protect the undulator against radiation damage. The undulator section consists of six undulators with a length of 4.5 m each.

For optimal FEL performance, the beam size in the undulator should not be increased by dispersive effects. The goal is to keep the contribution of these effects below 10%. The (dominant) energy spread generated during bunch compression in BC3 is about 0.3 MeV rms. Therefore, the dispersion generated between BC3 and the undulator must be corrected to less than 10 mm in both planes.

Dispersion correction also reduces undulator orbit launch sensitivity to rf amplitude and phase jitter. Inside the undulator section, the offsets of the (movable) quadrupole magnet centers are minimized.

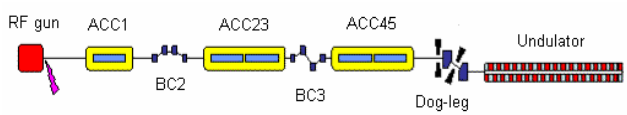

Figure 1: Schematic layout of FLASH

DISPERSION GENERATION

In a perfect lattice, dispersion is only generated in the bending magnets. However, any type of additional dipole field, caused for instance by quadrupole misalignments, dipole error fields (i.e. non closed chicanes), field errors of quadrupole magnets in dispersive sections or coupler kicks, will generate spurious dispersion.

Simulations for FLASH have been performed with the code elegant [2] in order to analyze which of the dispersion generation mechanisms are important.

Table 1 shows the magnitude of error required to generate 10 mm of dispersion after the dog-leg for different imperfections. In the first column, errors in the entire lattice are considered, while in the second column only errors in the dog-leg are taken into account. These numbers indicate that quadrupole misalignments are the most important cause of spurious dispersion and that the dog-leg is a critical area in terms of dispersion generation.

Table 1: Dispersion Generation Sensitivities

Source	**Error (in all the lattice)**	**Error (only in the dog-leg)**	**Dispersion (after the dog-leg)**
Quad misalignment	17 μm	50 μm	10 mm
Dipole field error	0.25 %	5.0 %	
Quad field error	0.75 %	0.75 %	

DISPERSION MEASUREMENT

Dispersion measurement is based on measuring the orbit for different beam energies. We scan the gradient of the different accelerator modules in the machine and analyze the orbit changes downstream. Figure 2 displays an example of a dispersion measurement at a single BPM.

To compensate the kick produced by the module when its gradient is changed, an orbit correction is performed. Two correctors in each direction are used to restore the orbit in two BPMs just downstream of the module. In principle, the magnets between the BPMs have to be scaled with beam energy while restoring offset and angle at the 2nd BPM [3], but for these measurements this effect can be neglected.

The (horizontal) orbit readings downstream of the 2nd BPM can be expressed as

$$x(s) = x_0(s) + R_{16}(s_0, s)\frac{\Delta p}{p} + R_{166}(s_0, s)\left(\frac{\Delta p}{p}\right)^2 + \ldots$$

where s_0 is the position of the 2nd BPM used for orbit correction after the module and s that of any other BPM. The R_{16} and R_{166} values are derived with a second order fit to the BPM data (see Figure 2). R_{16} is referred to as dispersion in this paper.

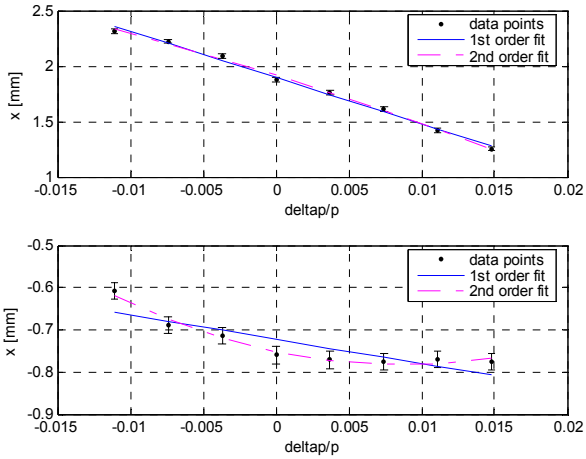

Figure 2: Dispersion at a single BPM

Figure 3 shows an example for a dispersion measurement along the machine. The energy was varied at ACC1 and the orbit corrected downstream of BC2. The plot shows $R_{16}(s)$ and $R_{36}(s)$ up to the undulator, where values of about 20 mm in the horizontal plane and more than 100 mm in the vertical were observed.

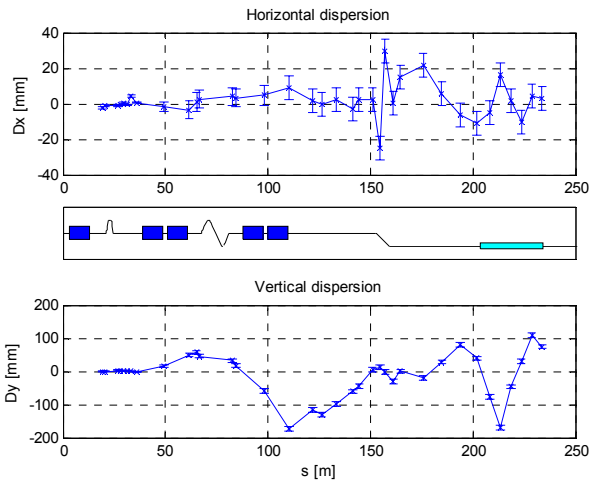

Figure 3: Example of R_{16} and R_{36} measurement

DISPERSION CORRECTION

Both orbit and dispersion can be simultaneously corrected using correction coils in the linac and quadrupole movers in the undulator region. The optimal settings are calculated using the orbit and dispersion response matrices, which are defined as the shift of the orbit or dispersion due to a change of corrector strength:

$$O_{i,j} = \frac{\Delta x_i}{\Delta \theta_j} \qquad D_{i,j} = \frac{\Delta D_i}{\Delta \theta_j}$$

where Δx_i and ΔD_i is the change of the orbit and dispersion in the BPM i, and $\Delta\theta j$ is the change of the strength of the corrector j.

The resulting orbit and dispersion change due to a change in corrector strength is given by:

$$\begin{pmatrix} \underline{\underline{O}} \cdot (1-w) \\ \underline{\underline{D}} \cdot w \end{pmatrix} \cdot \underline{\Delta\theta} = \begin{pmatrix} \underline{x} \cdot (1-w) \\ \underline{d} \cdot w \end{pmatrix},$$

where $\underline{\Delta\theta}$ is a vector of corrector strengths, $\underline{x}$ and $\underline{d}$ are respectively the orbit and dispersion and w is a factor that goes from 0 to 1 and defines the relative weight for orbit and dispersion correction. The algorithm finds a setting of correctors which minimizes the finally resulting orbit and dispersion:

$$(1-w)^2 \left\| \underline{x}_{meas} + \underline{\underline{O}} \cdot \underline{\Delta\theta} \right\|^2 + w^2 \left\| \underline{d}_{meas} + \underline{\underline{D}} \cdot \underline{\Delta\theta} \right\|^2 = \min$$

The dispersion correction procedure consists of four steps (see also Figure 4):

- measure the orbit for different energies
- derive average orbit and dispersion
- apply correction algorithm using the orbit and dispersion response matrices
- set the corrector currents and the quadrupole movers displacements

which, in a real machine, have to be iterated to overcome model and BPM imperfections.

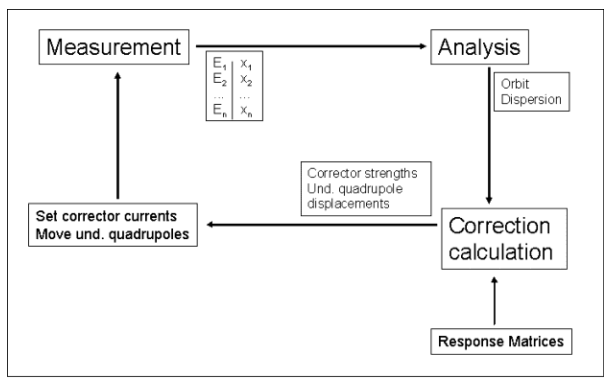

Figure 4: Dispersion correction procedure

Simulations

Figure 5 shows an example of a simulation of a global correction, using all the available correctors in the machine. The simulation takes into account the following machine imperfections: 100 µm quadrupole misalignment, 1% dipole and quadrupole field errors, a BPM noise of 20 µm, and BPM off-sets of 100 µm (all numbers rms). The upper and middle plots show orbit and dispersion along the machine before and after correction. The lower plot displays the change in corrector strengths and quadrupole mover positions required to perform the correction.

In this example the rms dispersion is reduced from 37 mm to 11.5 mm. Local correction in the undulator using the correctors downstream of the dog-leg yields a final rms dispersion of less than 5 mm in both planes.

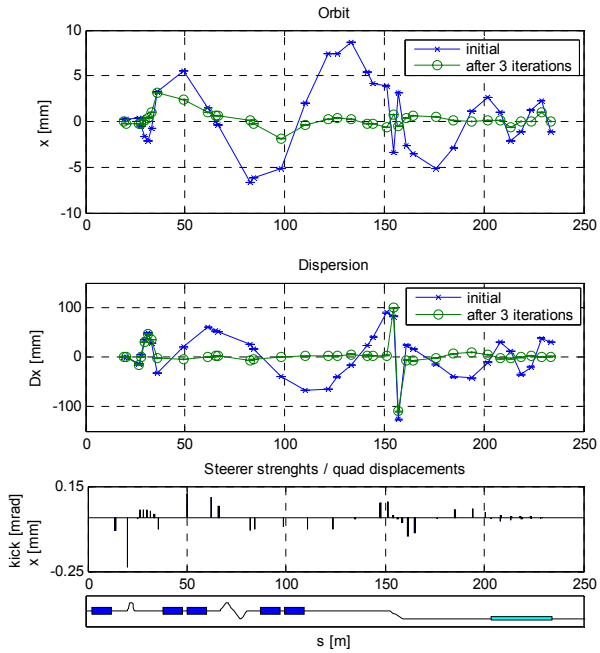

Figure 5: Example of simulated horizontal dispersion correction (downstream of ACC1)

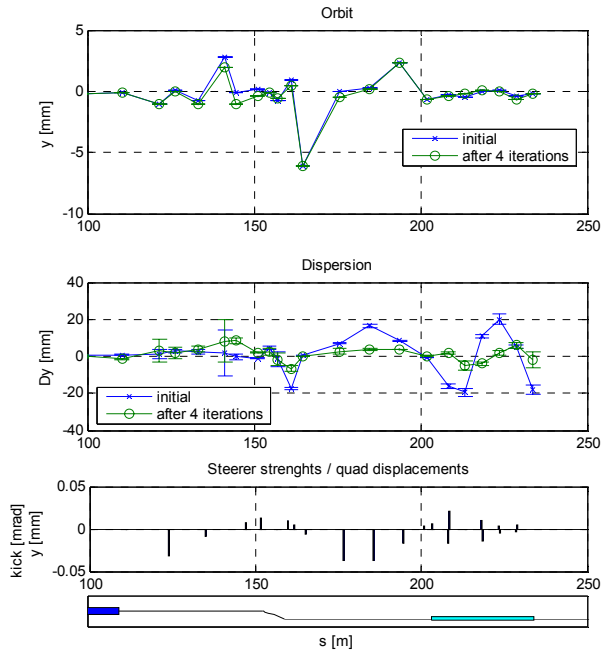

Figure 6: Example of measured vertical dispersion correction (downstream of ACC45)

Dispersion Correction Results

Figure 6 shows an example of dispersion measurement and correction in the vertical plane. The beam energy was varied in ACC45. The dispersion in the undulator was corrected while keeping the orbit constant. The rms dispersion was reduced from 17 mm to 4 mm after four iterations. The correction was done under lasing conditions. The projected emittance was reduced by about 25%, as measured with the wire scanners.

Dispersion measurement using ACC23 gave approximately the same values as with ACC45, which means that no dispersion was generated in the section between the two modules. However, when varying the beam energy with ACC1, dispersion of several centimetres was measured in the undulator region. This dispersion originates from the beam line section after the first bunch compressor.

CONCLUSIONS

A method for measuring and correcting the dispersion is presented. A tool has been developed and tested by means of simulations and measurements at FLASH at DESY.

We have corrected the dispersion in the undulator section. After correction, reduction of the projected beam emittance by around 25% has been observed. Complete dispersion compensation is still pending and expected to give more reduction in the undulator beam size.

REFERENCES

[1] J. Rossbach, “A VUV free electron laser at the TESLA test facility at DESY”, Nuclear Instruments and Methods in Physics Research Section A, Volume 375, p. 269-273 (1996).

[2] M. Borland, "elegant: A Flexible SDDS-Compliant Code for Accelerator Simulation", Advanced Photon Source LS-287, September 2000.

[3] P. Castro, “Orbit Correction by Dispersion Minimization in an Undulator with Superimposed FODO Lattice”, EPAC’98, Stockholm, June 1998, p. 658.

[4] T. Raubenheimer and R. Ruth, “A dispersion-free trajectory correction technique for linear colliders”, Nuclear Instruments and Methods in Physics Research Section A, Volume 302, Issue 2, p. 191-208 (1991).